J Chin Med Assoc

ORIGINAL ARTICLE

The effective distance and cooling rate of liquid nitrogen-based adjunctive cryotherapy for bone tumors ex vivo

Yu-Chuan Chang[a,b,c,d], Kuang-Yu Chao[c], Chao-Ming Chen[a,c,d,e], Cheng-Fong Chen[a,c,d,e], Po-Kuei Wu[a,c,d,e,*], Wei-Ming Chen[a,c,d,e]

[a]Department of Orthopedics and Joint Reconstruction, Taipei Veterans General Hospital, Taipei, Taiwan, ROC; [b]School of Medicine, Fu Jen Catholic University, Taipei, Taiwan, ROC; [c]Therapeutical and Research Center of Musculoskeletal Tumor, Taipei Veterans General Hospital, Taipei, Taiwan, ROC; [d]Institute of Clinical Medicine, School of Medicine, Yang Ming Chiao Tung University, Taipei, Taiwan, ROC; [e]Orthopedic Department of Medicine, National Yang Ming Chiao Tung University, Taipei, Taiwan, ROC

Abstract

Background: Liquid nitrogen (LN) has been used as an adjuvant cryotherapy for bone tumors including giant-cell tumor of the bone (GCTB) to remove residual tumor cells after curettage. This study evaluated variables related to the efficacy of LN-based cryoablation in the context of adjuvant treatment of GCTB using porcine femur bone model.

Methods: A porcine femur bone model was adopted to simulate intralesional cryotherapy. A LN-holding cavity (point 1, nadir) in the medial epicondyle, 4 holes (points 2–5) in the shaft situated 5, 10, 15, and 20 mm away from the proximal edge of the cavity, and 2 more holes (points 6 and 7) in the condyle cartilage (10 and 20 mm away from the distal edge of the cavity) were made. The cooling rate was compared between the 5 points. The cellular morphological changes and DNA damage in the GCTB tissue attributable to LN-based cryotherapy were determined by H&E stain and TUNEL assay. Cartilage tissue at points 6 and 7 was examined for the extent of tissue injury after cryotherapy.

Results: The temperature kinetics at points 1, 2 reached the reference target and were found to be significantly better than the reference (both $p < 0.05$). The target temperature kinetics were not achieved at points 4 and 5, which showed a significantly lower cooling rate than the reference (both $p < 0.001$) without reaching the –60°C target. Compared with untreated samples, significantly higher proportion of shrunken or apoptotic cells were found at points 1–3; very small proportion were observed at points 4, 5. Significantly increased chondrocyte degeneration was observed at point 6, and was absent at point 7.

Conclusion: The cryotherapy effective range was within 5 mm from nadir. Complications were restricted to within this distance. The cooling rate was unchanged after three repeated cycles of cryotherapy.

Keywords: Adjuvant therapy; Bone; Cryosurgery; Giant-cell tumor; Liquid nitrogen

1. INTRODUCTION

Extended curettage and wide resection are surgical options often used to treat bone tumors, and it has been shown that curettage alone exhibits better functional outcomes than wide resection.[1,2] However, extended curettage alone could result in residual tumor cells, which can potentially give rise to an increased risk of recurrence. For example, in giant-cell tumor of bone (GCTB), the recurrence rate has been reported to be as high as 31% after wide excision of unsalvageable limbs, but remained at approximately 8% after intralesional curettage.[3,4] As a result, adjunctive therapy using chemicals or cryogens have been adopted to control local recurrence in aggressive benign bone tumors, low-grade bone tumors, and metastatic bone tumors that had received curettage.[5–8]

Direct liquid nitrogen (LN) pouring is a conventional cryoablative method, however associated complications have been reported to be as high as 58% (30 of 52 patients) in an early pilot study.[8] Common complications associated with direct LN pouring are skin necrosis, neurovascular injury, infection, and pathological fracture.[8,9] Injury to surrounding tissue may occur due to direct contact with LN or radiant cooling.[10] Worth noting, cryotherapy can attenuate bone strength,[11] and cause postoperative pathologic fracture (range: 3.8% [1/26] to 6.5% [3/46]).[8,12,13] Combining cryotherapy with intralesional curettage, which interrupts the bone structure, may cause further bone damage. This has been demonstrated in a preclinical canine model.[14]

GCTB is a rare benign neoplasm predilected to occur in the long bones of young patients aged between 20 and 40 years.[15] GCTB can be aggressive and inflict pain, swelling, including in the joint, and pathological fracture.[16] Apart from the multinucleated osteoclast-like giant cells, stromal cells, and mononuclear

* Address correspondence. Dr. Po-Kuei Wu, Department of Orthopedics and Joint Reconstruction, Taipei Veterans General Hospital, 201, Section 2, Shi-Pai Road, Taipei 112, Taiwan, ROC. E-mail address: drwuvgh@gmail.com (P.-K. Wu).

Conflicts of interest: Dr. Wei-Ming Chen, an editorial board member at Journal of the Chinese Medical Association, had no role in the peer review process of or decision to publish this article. The other authors declare that they have no conflicts of interest related to the subject matter or materials discussed in this article.

Journal of Chinese Medical Association. (2022) 85: 866-873.

Received March 8, 2022; accepted March 29, 2022.

doi: 10.1097/JCMA.0000000000000761.

osteoclast precursor cells are also associated with GCTB.[16] Stromal cells have been found to remain and can potentially give rise to tumor recurrence after targeted therapy combined with surgery.[17] It is not known if the giant cells and stromal cells have different response patterns to adjunctive cryotherapy.

Previous reports have indicated that the nadir temperature, cooling rate, and the number of freeze-thaw cycles are the key factors associated with cryotherapy efficacy.[18] A lethal dose of cryoablation was previously defined as –20°C for 1 minute[19]; however, this temperature was later extended to –60°C to –70°C.[20,21] Bischof et al.[22] compared the effects of different cooling rates on tissue injury, and found that –20°C/min may be satisfactory. Intracellular and extracellular ice crystals formed during exposure to extreme cold are thought to disrupt cellular morphology and function.[23] It has been further acknowledged that the apoptotic response to temperature and morphological insults facilitate cellular destruction by cryotherapy.[18]

In the current report, we aim to address the effective range and cooling rate for LN-based cryoablation using GCTB excisional specimens embedded in porcine femur bone to simulate an intralesional cryotherapy ex vivo. The specific research questions were as follows: (1) What is the effective range and cooling rate by direct intralesional LN pouring to meet the demands of a successful cryoablation? (2) Will GCTB situated within the effective range of cryoablation be susceptible to tissue necrosis and cellular apoptosis? (3) Will the cartilage tissue situated close to the effective range of cryoablation be susceptible to damage or degeneration? (4) Will multiple freezing cycles improve the cooling rate and widen the effective range of freezing?

2. METHODS

2.1. GCTB excisional specimens

Cryotherapy simulation was performed on freshly processed surgical specimens from 3 patients with GCTB at our hospital (Taiwan, 2019). Clinical and histological information was obtained from patient charts and pathological reports (**Table 1**). Briefly, all 3 patients were in their thirties, with their tumor size ranging between 4.5 and 6 cm. None of the patient had received denosumab or bisphosphonate. All patients signed informed consent before the surgery and tissue collection. This study was approved by the institutional review board guidelines (approval no: 2019-02-021A) and conducted in accordance with the ethical statements in the Declaration of Helsinki.

2.2. Cryotherapy simulation and temperature recording

Before the experiment, a LN-holding cavity and 6 additional holes appropriately distanced away from the cavity were made in fresh porcine femurs purchased from a local slaughterhouse. A LN-holding cavity 40 (length) × 20 (width) × 30 (depth) mm was created on the medial epicondyle of the porcine femur by handheld electric drill. The residual trabecular bone was removed by handheld electric burr to ensure the volume of the cavity reached 24.0 mL. The LN-holding cavity was designated as point 1 and acted as the nadir of the cryotherapy simulation. Four holes (points 2–5) situated at 5, 10, 15, and 20 mm away from the proximal edge of the freezing cavity were made in the shaft, and 2 more holes (points 6 and 7) were made 10 and 20 mm away from the distal edge of the freezing cavity in the condyle cartilage (Fig. 1).

During the null cryotherapy simulation (ie, in the absence of GCTB tissues), temperature sensing probes were inserted into the 5 measuring points (ie, the cavity plus the 4 holes in the shaft) and the freezing cavity was filled (and maintained) to 80% capacity with fresh LN. The femur bone was left to stand for 10 minutes, during which the temperature on the 5 points was recorded every second by Paperless recorder VM7000A (Ohkura, Saitama, Japan). Cooling rates were derived from the temperature recordings. This was defined either as Δ°C/minute for the bone to reach –60°C or after 10 minutes since LN application, whichever came first. Previously, the target temperature and cooling rate required for successful cryotherapy had been established to be –60°C and –20°C/min, respectively.[20,22,24] This is visualized with dashed lines in **Figs. 2 and 6** and is used as the reference for minimal freezing requirements. Three porcine bones were utilized for the cryotherapy simulation.

To test the dynamics of multiple freeze-thaw cycles, the femur bone with the thermo probes in place were subjected to the indicated cycles consisting of one 10-minute freezing step and one 30-minute thawing step. In the efficacy validation experiment, the GCTB excisional specimen was collected and cut into appropriate size in order to fit into hollow copper tubes 3.0 mm in diameter. These tubes were used to transfer and hold the bone tumor tissue in place while measuring points 1–5 described above. A fresh porcine bone was utilized when a new patient specimen was available. The GCTB tissue placed in the femur bone was then subjected to 5 minutes of freezing by LN directly poured into the cavity (point 1) followed by 30 minutes of thawing according to previously described methods.[7] GCTB tissue exposed to freeze-thaw cryoablation was extracted from the bone and fixed with 4% paraformaldehyde. The cellular morphological changes and DNA damage were examined by Hematoxylin and Eosin (H&E) stain, and terminal deoxynucleotidyl transferase dUTP nick end labeling (TUNEL) assay, respectively. Porcine cartilage samples were also exposed to control treatment in LN. Those samples collected from points 6 and 7 were tested using safranin O and Fast Green stain to identify microscopic cartilage changes.

2.3. H&E stain

Sections of 3 μm were prepared from paraffin-embedded tissue blocks and stained using commercial hematoxylin and eosin reagents (Sigma-Aldrich, NJ). Briefly, slides were deparaffinized and processed as follows: incubation at 75°C in an oven for 10 minutes; three 5-minute rinses in xylene; three 5-minute rinses in 100% ethanol; one 5-minute rinse in each of the 95% ethanol, 75% ethanol, and 50% ethanol solutions, consecutively; one 3-minute rinse in running tap water; one 5-minute staining incubation immersed in Mayer's hematoxylin solution. Slides were then rinsed once in running cold tap water for 5 minutes, 10 times in 95% acid ethanol for 3 second each and stained in eosin Y solution for 30 seconds. Slides were dehydrated by one 3-minute immersion in each of the 50% ethanol, 75% ethanol, and 95% ethanol solutions, and three 3-minute immersions in 100% ethanol, and cleared in three 3-minute immersions in xylene. Data from 5 representative nonoverlapping fields selected under 400× magnification were pooled for each clinical specimen.

Table 1

Profile of patients with giant-cell tumor

	Case 1	Case 2	Case 3
Age	30	35	33
Gender	Male	Male	Female
Location	Distal femur	Proximal tibia	Distal femur
Size (cm)	5	4.5	6
Stage	II	III	II
Use of denosumab	No	No	No
Use of bisphosphonate	No	No	No

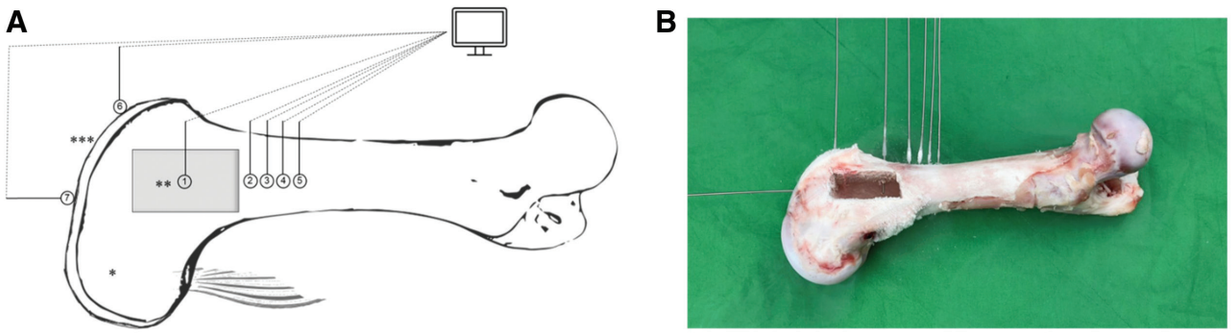

Fig. 1 Schematic figure showing the locations of the 7 observation points A. Point 1: control, freezing cavity. Point 2: bone_d_5 mm, the point in bone marrow 5 mm distant from the edge of freezing cavity; Point 3: bone_d_10 mm, the point in bone marrow 10 mm distant from the edge of freezing cavity; Point 4: bone_d_15 mm, the point in bone marrow 15 mm distant from the edge of freezing cavity; Point 5: bone_d_20 mm, the point in bone marrow 20 mm distant from the edge of freezing cavity; Point 6: cartilage_d_10 mm, the point in cartilage 10 mm distant from the edge of freezing cavity; Point 7: cartilage_d_20 mm, the point in cartilage 20 mm distant from the edge of freezing cavity. *Distal porcine femur bone; **Freezing cavity, 40 mm in length, 20 mm in width, and 30 mm in depth; ***Articular cartilage over distal femur. Temperature kinetics of points 1–5 were derived continuously from recordings during cryotherapy.

2.4. TUNEL assay

Genomic DNA fragmentation resulting from an apoptotic signaling cascade was detected using a TUNEL assay (In Situ Cell Death Detection kit; Roche, Basel, Switzerland).[25] To identify TUNEL signals specific to giant cells and stromal cells in the GCTB tissue, the cellular nuclei were counterstained using 4,6-diamidino-2-phenylindole (DAPI). Slides were covered with glass slips and code-labeled for blinded evaluation using an Olympus BX41 microscope (Olympus, Tokyo, JP). Data from 5 representative nonoverlapping fields selected under 400× magnification were pooled for each specimen.

2.5. Safranin O/Fast Green stain for cartilage

Sections of 3 μm were prepared from paraffin-embedded tissue blocks and stained using safranin O or Fast Green and counterstained using hematoxylin.[26] Briefly, slides were deparaffinized and processed following the same procedures as in H&E staining up to the hematoxylin step, followed by slides were then rinsed once in running cold tap water for 2 minutes, stained with 0.08% Fast Green for 2 minutes, immersed in 1.0% acetic acid for 10 seconds, stained with 0.1% safranin O solution for 5 minutes, dipped in 0.5% acetic acid, and rinsed for 5 minutes under running water. Slides were air dried and covered with glass slips. Data from 5 representative nonoverlapping fields selected under 400× magnification were pooled for each specimen.

2.6. Data presentation and statistical analysis

Slides were covered with glass slips and coded for blinded evaluation before evaluation using an Olympus BX41 microscope (Olympus, Tokyo, JP). Cell counts from 5 randomly selected nonoverlapping fields viewed under 400× magnification were analyzed. All data are presented as mean ± SD. One-way ANOVA was used to analyze the cooling rates and cellular counts from the various staining assays. Two-way ANOVA was used to analyze the cooling rate between three tests.

3. RESULTS

3.1. The kinetics of temperature change in different points of the femur bone during LN-based cryotherapy

To evaluate the effective distance and cooling rate of intralesional LN-based cryotherapy, a simulation model using porcine femur bones was established as described in the Materials and Methods and schematically shown in **Fig. 1**. The kinetics of temperature change at the indicated points in the porcine femur bone were recorded and are presented in **Fig. 2**.

At point 1 (freezing cavity, nadir), the temperature dropped to –60°C within 6 seconds, indicating a cooling rate of –1330.8 ± 427.9°C. At point 2 (situated in the shaft and 5 mm away from the proximal edge of the cavity; bone_d_5 mm), the temperature dropped to –60°C in 93 seconds, indicating a cooling rate of –55.7 ± 16.7°C. The target temperature was achieved

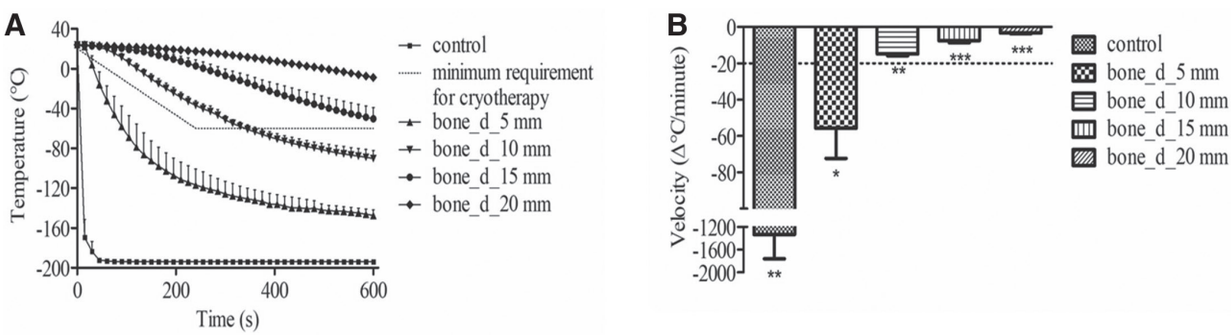

Fig. 2 Temperature kinetics during the 10-minute cryotherapy simulation. (A) The temperature change over time at control, bone_d_5, 10, 15, and 20 mm (n = 3). (B), the cooling rate (velocity) of indicated points in the porcine femur bone (n = 3); the velocity was derived from the period from 0 seconds to the time point when the temperature reached –60°C or the period from 0 to 600 seconds (10 minutes) if the temperature d not reach –60°C and expressed as Δ°C/minute. The reference values (dotted line) showing the minimum requirement for cryotherapy was plotted in accordance with the published data.[22]

at points 1 and 2, and the cooling rates at each point were significantly greater than the reference (p = 0.006 and 0.021, respectively).

At point 3 (situated in the shaft 10 mm away from the proximal edge of the cavity; bone_d_10 mm), the temperature reached the −60°C target in 340 seconds, indicating a cooling rate of −14.8 ± 1.1°C. In contrast, the target temperature (−60°C) was not reached within the observation period (600 seconds) at points 4 (bone_d_15 mm) and 5 (20 mm). The cooling rates at points 4 and 5 were −7.5 ± 1.2°C and −3.3 ± 0.4°C, respectively. The cooling rates at points 3–5 were all significantly lower than the reference (all p < 0.001), suggesting that the effect of cryoablation may be reduced at distant sites. We subsequently tested the temperature kinetics in porcine femur bones exposed to multiple freeze-thaw cycles of intralesional LN-based cryotherapy simulation. Furthermore, the efficacy of LN-based cryoablation were then validated using freshly collected GCTB specimens.

3.2. Cellular morphological changes after cryotherapy

Cryotherapy results in tumor cell shrinkage and injury,[27] which then activates the cascade of cellular apoptosis.[28,29] The H&E stain was used to evaluate the morphological and histological changes in the GCTB tissue after cryotherapy (**Fig. 3A**).

The proportion of giant cells that displayed cellular shrinkage in untreated samples (unexposed to cryotherapy, 0.4% ± 0.7%) compared with samples treated at point 1 (control, 24.3% ± 3.7%) and point 2 (bone_d_5 mm, 18.4% ± 6.3%) was significantly higher (both p < 0.001). The proportion of shrunken giant cells in samples treated at point 3 (bone_d_10 mm, 13.2% ± 8.3%) was also significantly higher than that in the untreated samples (p = 0.002). The proportion of giant cells that underwent cellular shrinkage in samples treated at point 4 (bone_d_15 mm, 2.4% ± 2.5%) and point 5 (bone_d_20 mm, 0% ± 0%) showed no significant difference compared with the untreated group (p = 0.058 and p = 0.081, respectively) (**Fig. 3B**). Based on the histology examination, point 3 was exposed to some cryoablation compared with points 1 and 2, whereas points 4 and 5 received limited cryoablative activity derived from LN.

3.3. DNA damage and apoptotic changes after cryotherapy

TUNEL stain was used to confirm the DNA damage and cellular apoptosis,[25] and DAPI staining was used to identify giant cells (indicated by yellow-dashed lines in **Fig. 4A**) from stromal cells.

All giant cells and stromal cells were undergoing apoptosis (stained green by TUNEL) in samples treated at point 1 (control; 100%) or point 2 (bone_d_5 mm; 100%) after cryotherapy. This was significantly increased compared with untreated samples (0%, both p < 0.001). Although the proportion of TUNEL positive giant cells (30.3% ± 11.0%) and stromal cells (8.3% ± 2.4%) in samples treated at point 3 (bone_d_10 mm) were lower than those at points 1 and 2, they were significantly higher than those in the untreated samples (p = 0.02 and p < 0.001, respectively). No apoptotic signals were observed in samples treated at points 4 and 5 (**Fig. 4B**,C).

Consistency between the TUNEL results and histology findings further demonstrate that giant cells in samples treated at points 1 and 2 had undergone apoptosis regardless of the presence of a shrunken appearance, which may be more reflective of the cooling rate rather than target temperature.

3.4. Cartilage changes after cryotherapy

Safranin O and Fast Green staining reveals the smoothness of the cartilage surface and also cartilage cavity size that can be translated into the extent of chondrocyte degeneration.

As illustrated by representative micrographs in **Fig. 5A**, the cartilage surface of all samples appeared smooth, and no differences were observed between samples. The chondrocyte degeneration rate was significantly increased in the cartilage exposed directly to LN (control, 15.7% ± 18.9%) and in the cartilage at point 6 (cartilage_d_10 mm, 8.3% ± 14.9%) compared with untreated cartilage (0.6% ± 4.5%; both p < 0.001). No significant change was observed between cartilage at point 7 (cartilage_d_20 mm, 1.3% ± 5.6%) and the untreated samples (0.6% ± 4.5%, p = 0.266) (**Fig. 5B**). Therefore, despite the target cooling rate was not achieved 10 mm away from point 1, which was exposed to LN directly, and the cartilage situated a similar distance to LN was injured to some extent.

3.5. Cooling rate after repeated cryotherapy

The temperature kinetics at points 2–5 during each of the 3-consecutive cryotherapy freeze-thaw cycles did not indicate a significant change in the cooling rates (**Fig. 6**). The temperature kinetics curves at points 4 and 5 remained above the reference (**Fig. 6C**,D), although the target temperature was reached in the last few seconds of the second and third cycles at point 4. This result implies limitations associated with additional freeze-thaw cycles (eg, unwanted tissue injury) in terms of enhancing cryoablative activity.

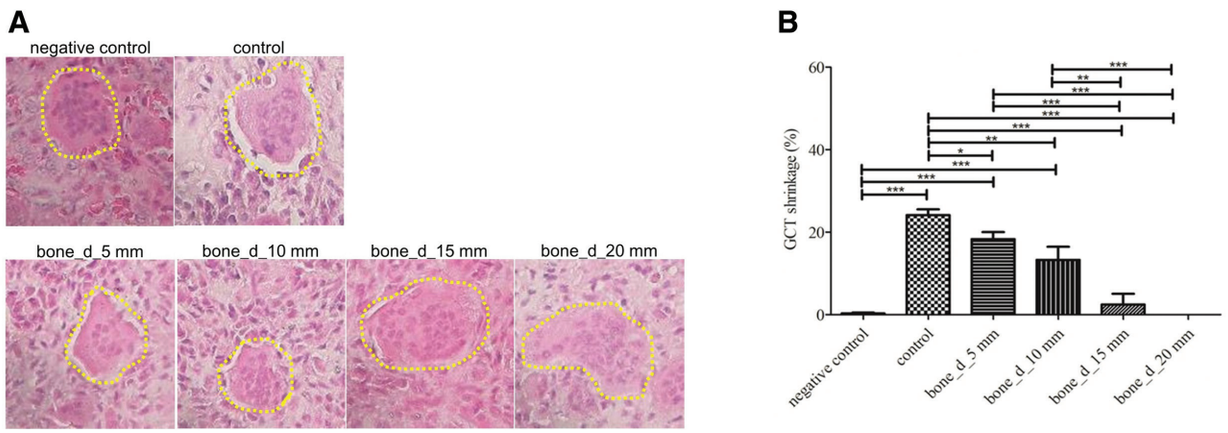

Fig. 3 H&E stain after cryotherapy. (A) Representative micrographs (400×) taken from specimens (n = 3) in the negative control, control, bone_d_5 mm, bone_d_10 mm, bone_d_15 mm, and bone_d_20 mm groups. (B) Histogram of GCT cell shrinkage, data presented as mean ± standard deviation (n = 3 clinical specimens, *p < 0.05, **p < 0.01, and ***p < 0.001).

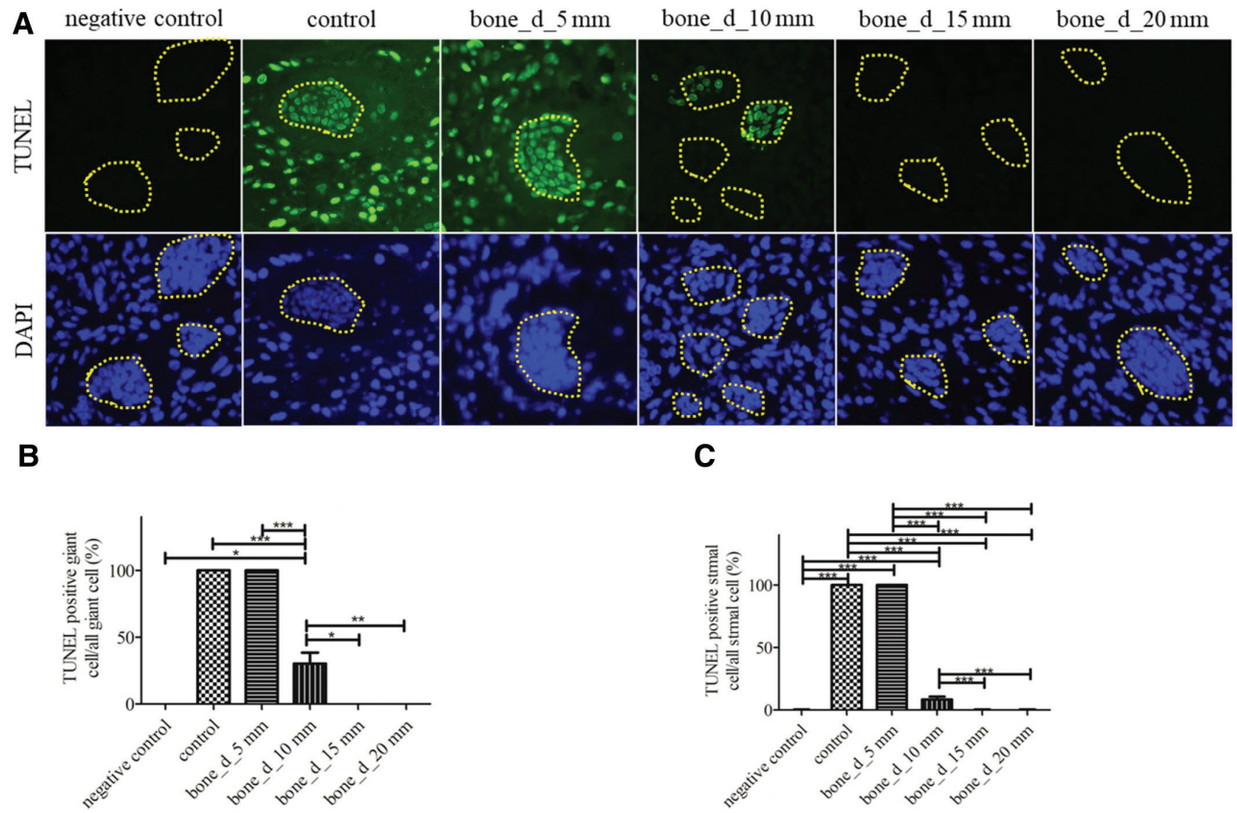

Fig. 4 The proportion of apoptotic cells after cryotherapy. Clinical specimens (n = 3) in each of the treatment groups were stained by TUNEL assay and DAPI; (A) representative micrographs (400×) taken from specimens in the negative control, control, bone_d_5 mm, bone_d_10 mm, bone_d_15 mm, and bone_d_20 mm groups, where giant cells were marked by yellow broken lines; histograms of apoptotic giant cells. (B) and stromal cells (C) (n = 3 clinical specimens, $^{*}p < 0.05$, $^{**}p < 0.01$, and $^{***}p < 0.001$).

4. DISCUSSION

4.1. Although intralesional curettage is a common treatment choice for various bone tumors, it is associated with a high recurrence rate

Intralesional curettage is an important surgical management tool for local aggressive bone tumors such as a GCTB or low-grade chondrosarcoma. Li et al.[30] reported a local recurrence rate after intralesional curettage of 41.9% in 179 patients treated for GCTB between 1998 and 2010. A separate study indicated that the rates of local and metastatic recurrence in GCTB ranged from 8% to 62% and 1.5% to 7%, respectively.[31] Surgical treatment in aggressive bone tumors remains challenging, and many adjunctive therapies have been utilized to reduce the risk of recurrence.

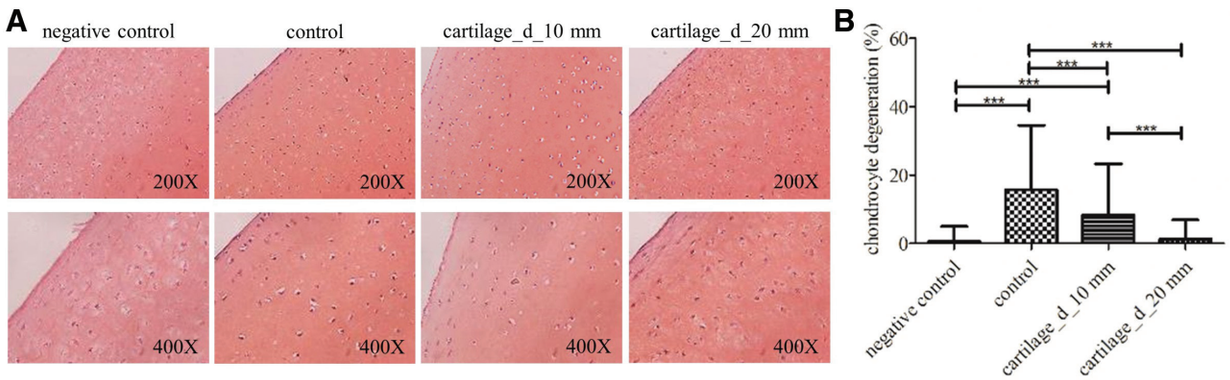

Fig. 5 Cartilage changes after cryotherapy. Porcine cartilage tissue (n = 3) subjected to cryotherapy were stained by safranin O and Fast Green stain to demonstrate changes in the smooth surface and lacuna space, (A) representative micrographs (400×) taken from specimens (n = 3) in the negative control, control, bone_d_5 mm, bone_d_10 mm, bone_d_15 mm, and bone_d_20 mm groups. (B) Histogram of shrunken area of lacuna (%); data are presented as mean ± standard deviation. $^{*}p < 0.05$, $^{**}p < 0.01$, and $^{***}p < 0.001$. There was no difference in surface and width of cartilage in all groups.

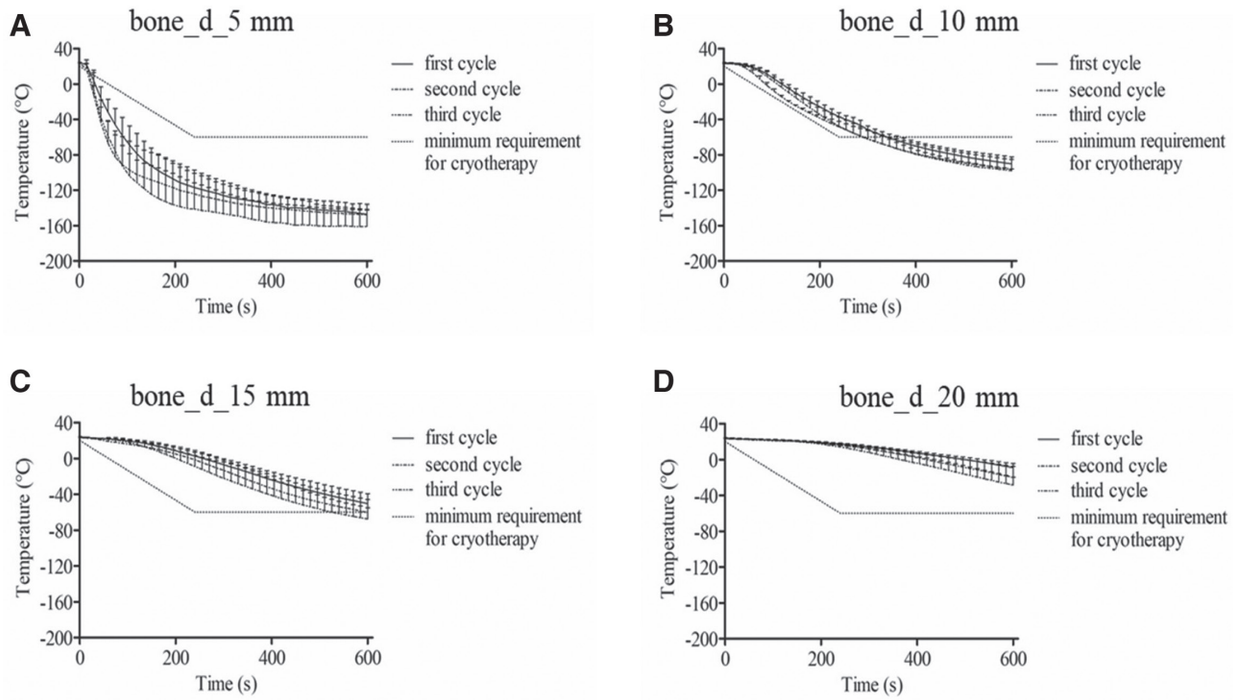

Fig. 6 Temperature kinetics over the 3-consecutive cycles of 10-minute cryotherapy. Temperature changes recorded at bone_d_5 mm (A), bone_d_10 mm (B), bone_d_15 mm (C), and bone_d_20 mm (D). The reference curve (dotted line) showing the minimum requirement for cryotherapy was plotted in accordance with the published data. Data are presented as mean ± standard deviation (n = 3 porcine femur bones). Two-way ANOVA analysis was utilized, and no significant differences were found in any of the groups.

4.2. Adjunctive therapies including phenol and cryotherapy have been utilized to decrease the risk of recurrence

Adjuvant therapy such as phenol or cryotherapy with LN have been used to lower local recurrence rate. Capanna et al.[32] reported a 7% local recurrence rate in 165 benign bone tumors treated with curettage followed by the application of phenol. Mittag et al.[6] reported that phenol at a concentration of 60% to 80% may not be suitable for the treatment of remaining solid tissue of giant-cell tumors due to the penetration depth being low at up to 100 μm maximally. More solid tumors may exhibit septum or sclerotic chambers that can be problematic for tumor removal in upper or distant chambers regardless of prior curettage or phenol use. Trieb et al.[33] revealed the local recurrence rate of giant-cell tumors treated with or without phenol was comparable. Meanwhile, LN has also gained acceptance as an agent for cryotherapy as pioneered by Tsuchiya et al.[34] for the purpose of biomechanical reconstruction. To improve upon the limitations associated with LN-based cryotherapy, freezing nitrogen ethanol composite has been proposed and tested clinically as a cryogen for adjuvant therapy to clear the remaining tumor cells after curettage.[7]

4.3. The critical role of cryotherapy effective range

Due to the potential presence of a septum or sclerotic chamber in a bone tumor that are more solid in structure, the effective range or depth of cryotherapy is critical for treatment success. The lethal temperature and cooling rate for tumor eradication have been established to be –60°C and –20°C/minute, respectively.[20,22] This was used as a basis for determining the effective range of cryotherapy. Our cryotherapy simulation study found that both the target temperature and cooling rate were achieved only within a depth of 5 mm, whereas the result from the TUNNEL assay revealed a sharp decrease in giant-cell apoptosis from 100% to 30% at 10 mm, indicating that the tumor-killing capacity of cryotherapy may be limited beyond a distance of 10 mm. On the other hand, the apoptosis rate of stromal cells at 10 mm was only 8.3%, indicative of relatively little apoptotic activity in this population. This observation also suggests that GCTB stromal cells may be protected from LN-based cryotherapy at 10 mm. Therefore, these results suggest that tumor cell eradication can be achieved by LN pouring for 10 minutes at an effective depth of 5 mm, and that the tumor-killing activity is gradually lost between 5 and 10 mm in depth, in contrast to the 100 μm penetration demonstrated by phenol.[6] We suggest that careful removal of all visible tumor and a breakage of the intralesional sclerotic septum are vital for bone tumor surgeries involving curettage. Prolonged cryotherapy may be an option to extend the effective distance or reach at a lower temperature, but our study found that at 10 mm away from the nadir, the target temperature was reached without a sufficient cooling rate, which translated into decreased tumor-killing activity. Moreover, LN will need to be replenished during prolonged cryotherapy, increasing the likelihood of unwanted spillage or overflow that may damage the surrounding tissue.

4.4. The range of cartilage damage during cryotherapy

The complication rate associated with direct LN pouring has been reported to range from 0% to 21% (Clinical experience of freezing nitrogen ethanol composite in treating bone tumors: a short-term follow-up, manuscript under review). The cause of complications may be LN spillage during transport, LN overflow due to breakthrough in the cortical bone, or radiant cooling originating from LN. Tumor lesions often occur in the epiphysis close to the joint, and when the tumor margin is close to the joint cryotherapy-derived cartilage damage becomes a clinical

concern for surgeons. In the current study, the condyle cartilage in the porcine femur was utilized to demonstrate potential tissue damage from radiant cooling. We found that the cartilage tissue at 10 or 20 mm, which is beyond the effective cryoablation range indicated earlier, showed tissue integrity comparable to that of untreated samples. However, increased lacuna shrinkage suggesting chondrocyte degeneration was noted upon safranin O/Fast Green stain at 10 mm away from nadir compared with untreated samples. Cartilage may only be partially protected from radiant cooling when situated 10 mm away during cryotherapy. Hence, sufficient protective measures such as warm water irrigation or warm pad protection to keep the surrounding normal tissue warm are pivotal. Additional care and attention should be given to neurovascular bundles within 10 mm from the cryotherapy nadir.

4.5. The effects of repeated cryotherapy

It has been proposed that increased cellular apoptosis and tumor-killing could be achieved by using repeated bouts of cryotherapy. During cryotherapy, the structure of the bone may be altered, leading to enhanced radiant cooling. In our study, we found that repeated freeze-thaw cycles did not lead to a notable change in the lowest temperature reached or cooling rate from nadir to 20 mm away. Nevertheless, our study was unable to exclude the possibility of cellular membrane disruption by additional crystallization formed after repeated cryotherapy and this may contribute to increased tumor necrosis that has been hypothesized by others.[24]

The current study demonstrated the effective range and cooling rate of LN-based cryotherapy via an ex vivo simulation using porcine femur bones. Porcine femurs were chosen based on their availability and similar size compared with humans; however, it is worth noting that porcine femurs differ from human bones in gross and microscopic anatomy. Furthermore, the size of tumors is always different in the clinical setting, and only one type of cavity was tested in the current study. In real-world scenarios, the continued vascular perfusion of the tumor lesion and the affected limb may influence the outcomes of cryotherapy, and vascular perfusion was unfortunately absent in the present simulation model, and the actual effect of blood supply would need to be investigated in future studies. We suggest the use of a tourniquet to prevent blood flow from disrupting the effective range and cooling rate associated with of cryotherapy.

In conclusion, the cryotherapy effectiveness of direct LN pouring sustained within a depth of 5 mm away from nadir. Tumor apoptotic activity was partially observed between 5 and 10 mm away from nadir. An intermediate protection for cartilage could be achieved at 10 mm. The effective range and cooling rate were not altered after three cycles of cryotherapy. The results should provide several points worthy of consideration for clinical decision making during intralesional or adjunctive cryotherapy. The extrapolation of the current findings should be validated in real-world settings.

ACKNOWLEDGMENTS

This work was supported by grants from the Veterans General Hospital-Taipei (V104C-001) and kindly financial supported by Dr. Morris Chang and Ms. Sophie Chang.

REFERENCES

1. Chen X, Yu LJ, Peng HM, Jiang C, Ye CH, Zhu SB, et al. Is intralesional resection suitable for central grade 1 chondrosarcoma: a systematic review and updated meta-analysis. *Eur J Surg Oncol* 2017;**43**:1718–26.
2. Chen YC, Wu PK, Chen CF, Chen WM. Intralesional curettage of central low-grade chondrosarcoma: a midterm follow-up study. *J Chin Med Assoc* 2017;**80**:178–82.
3. Liu YP, Li KH, Sun BH. Which treatment is the best for giant cell tumors of the distal radius? a meta-analysis. *Clin Orthop Relat Res* 2012;**470**:2886–94.
4. Pazionis TJ, Alradwan H, Deheshi BM, Turcotte R, Farrokhyar F, Ghert M, et al. A systematic review and meta-analysis of en-bloc vs intralesional resection for giant cell tumor of bone of the distal radius. *Open Orthop J* 2013;**7**:103–8.
5. Dürr HR, Maier M, Jansson V, Baur A, Refior HJ. Phenol as an adjuvant for local control in the treatment of giant cell tumour of the bone. *Eur J Surg Oncol* 1999;**25**:610–8.
6. Mittag F, Leichtle C, Kieckbusch I, Wolburg H, Rudert M, Kluba T, et al. Cytotoxic effect and tissue penetration of phenol for adjuvant treatment of giant cell tumours. *Oncol Lett* 2013;**5**:1595–8.
7. Wu PK, Chen CF, Wang JY, Chen PC, Chang MC, Hung SC, et al. Freezing nitrogen ethanol composite may be a viable approach for cryotherapy of human giant cell tumor of bone. *Clin Orthop Relat Res* 2017;**475**:1650–63.
8. Marcove RC, Weis LD, Vaghaiwalla MR, Pearson R, Huvos AG. Cryosurgery in the treatment of giant cell tumors of bone. a report of 52 consecutive cases. *Cancer* 1978;**41**:957–69.
9. Chen C, Garlich J, Vincent K, Brien E. Postoperative complications with cryotherapy in bone tumors. *J Bone Oncol* 2017;**7**:13–7.
10. Chen CF, Chu HC, Chen CM, Cheng YC, Tsai SW, Chang MC, et al. A safety comparative study between freezing nitrogen ethanol composite and liquid nitrogen for cryotherapy of musculoskeletal tumors. *Cryobiology* 2018;**83**:34–9.
11. Fisher AD, Williams DF, Bradley PF. The effect of cryosurgery on the strength of bone. *Br J Oral Surg* 1978;**15**:215–22.
12. Mohler DG, Chiu R, McCall DA, Avedian RS. Curettage and cryosurgery for low-grade cartilage tumors is associated with low recurrence and high function. *Clin Orthop Relat Res* 2010;**468**:2765–73.
13. Schreuder HW, Veth RP, Pruszczynski M, Lemmens JA, Koops HS, Molenaar WM. Aneurysmal bone cysts treated by curettage, cryotherapy and bone grafting. *J Bone Joint Surg Br* 1997;**79**:20–5.
14. Malawer MM, Marks MR, McChesney D, Piasio M, Gunther SF, Schmookler BM. The effect of cryosurgery and polymethylmethacrylate in dogs with experimental bone defects comparable to tumor defects. *Clin Orthop Relat Res* 1988;299-310.
15. Liede A, Bach BA, Stryker S, Hernandez RK, Sobocki P, Bennett B, et al. Regional variation and challenges in estimating the incidence of giant cell tumor of bone. *J Bone Joint Surg Am* 2014;**96**:1999–2007.
16. Lipplaa A, Dijkstra S, Gelderblom H. Challenges of denosumab in giant cell tumor of bone, and other giant cell-rich tumors of bone. *Curr Opin Oncol* 2019;**31**:329–35.
17. van der Heijden L, Dijkstra S, van de Sande M, Gelderblom H. Current concepts in the treatment of giant cell tumour of bone. *Curr Opin Oncol* 2020;**32**:332–8.
18. Baust JG, Bischof JC, Jiang-Hughes S, Polascik TJ, Rukstalis DB, Gage AA, et al. Re-purposing cryoablation: a combinatorial 'therapy' for the destruction of tissue. *Prostate Cancer Prostatic Dis* 2015;**18**:87–95.
19. Cooper IS. Cryobiology as viewed by the surgeon. *Cryobiology* 1964;**51**:44–51.
20. Neel HB 3rd, Ketcham AS, Hammond WG. Requisites for successful cryogenic surgery of cancer. *Arch Surg* 1971;**102**:45–8.
21. Staren ED, Sabel MS, Gianakakis LM, Wiener GA, Hart VM, Gorski M, et al. Cryosurgery of breast cancer. *Arch Surg* 1997;**132**:28–33.
22. Bischof J, Christov K, Rubinsky B. A morphological study of cooling rate response in normal and neoplastic human liver tissue: cryosurgical implications. *Cryobiology* 1993;**30**:482–92.
23. Maccini M, Sehrt D, Pompeo A, Chicoli FA, Molina WR, Kim FJ, et al. Biophysiologic considerations in cryoablation: a practical mechanistic molecular review. *Int Braz J Urol* 2011;**37**:693–6.
24. Gage AA, Baust J. Mechanisms of tissue injury in cryosurgery. *Cryobiology* 1998;**37**:171–86.
25. Charriaut-Marlangue C, Ben-Ari Y. A cautionary note on the use of the tunel stain to determine apoptosis. *Neuroreport* 1995;**7**:61–4.
26. Schmitz N, Laverty S, Kraus VB, Aigner T. Basic methods in histopathology of joint tissues. *Osteoarthritis Cartilage* 2010;**18** Suppl 3:S113–6.
27. Hanai A, Yang WL, Ravikumar TS. Induction of apoptosis in human colon carcinoma cells ht29 by sublethal cryo-injury: mediation by cytochrome c release. *Int J Cancer* 2001;**93**:526–33.

28. Pegg DE, Diaper MP. On the mechanism of injury to slowly frozen erythrocytes. *Biophys J* 1988;**54**:471–88.
29. Yiu WK, Basco MT, Aruny JE, Cheng SW, Sumpio BE. Cryosurgery: a review. *Int J Angiol* 2007;**16**:1–6.
30. Li D, Zhang J, Li Y, Xia J, Yang Y, Ren M, et al. Surgery methods and soft tissue extension are the potential risk factors of local recurrence in giant cell tumor of bone. *World J Surg Oncol* 2016;**14**:114.
31. Kremen TJ Jr, Bernthal NM, Eckardt MA, Eckardt JJ. Giant cell tumor of bone: are we stratifying results appropriately? *Clin Orthop Relat Res* 2012;**470**:677–83.
32. Capanna R, Sudanese A, Baldini N, Campanacci M. Phenol as an adjuvant in the control of local recurrence of benign neoplasms of bone treated by curettage. *Ital J Orthop Traumatol* 1985;**11**:381–8.
33. Trieb K, Bitzan P, Lang S, Dominkus M, Kotz R. Recurrence of curetted and bone-grafted giant-cell tumours with and without adjuvant phenol therapy. *Eur J Surg Oncol* 2001;**27**:200–2.
34. Tsuchiya H, Wan SL, Sakayama K, Yamamoto N, Nishida H, Tomita K, et al. Reconstruction using an autograft containing tumour treated by liquid nitrogen. *J Bone Joint Surg Br* 2005;**87**:218–25.